cRGD Nanoparticles Loaded with Microbubbles for Enhancing Anti-Proliferation and Anti-Angiogenesis

Xia Zhang
University of South China
Rongping Xie
Shaoyang Central Hospital
Zhixiong Luo
University of South China
Haihong Liao
University of South China
Da Ouyang
University of South China
Man Chen
University of South China
Bing Zhou (xatodm@163.com)
University of South China

Research Article

Keywords: cRGD Nano, Ultrasound, endothelium-dependent vessels, vasculogenic mimicry

Posted Date: February 16th, 2022

DOI: https://doi.org/10.21203/rs.3.rs-1348985/v1

Abstract

Background: The inhibition of angiogenesis leads to the degeneration of tumors; thus, anti-angiogenesis therapy is a strategy for the treatment of tumors. Accumulating documents has demonstrated effective anti-angiogenic strategies should simultaneously inhibit endothelium-dependent vessels (EDV) and tumor cell-mediated vasculogenic mimicry (VM). Although cRGD peptide enabling to bind with a_vb_3 integrin can specifically inhibit both EDV and VM, however peptide-based drug delivery platforms have not obtained the expected therapeutic efficacy due to their rapid degradation and low tumor accumulation.

Results: Herein, we developed cRGD nanoparticles (cRGD Nano) loaded microbubbles (MB) to enhance their anti-EDV and anti-VM ability for endothelial cells and ovarian cancer cells due to the sonoporation effect from ultrasound (US). Heparin as backbone conjugated with cRGD to prepare cRGD-H conjugate and then loaded with biotin thereby following dialysis to fabricate cRGD Nano. Subsequently, the cRGD Nano were incorporated with MB via avidin-biotin linkage to fabricate cRGD Nano-MB. The enhanced anti-angiogenic effect can take profit of cRGD from cRGD Nano and sonoporation effect from US combined with MB. cRGD Nano has been characterized, and cRGD Nano-MB combined with US exhibited the best intracellular uptake ability than cRGD Nano and cRGD Nano-MB without US by flow cytometry and confocal laser scanning microscopy. Also, cRGD Nano-MB combined with US could efficiently discourage the tube formation of endothelial cells and cancer cells, and presented excellent significant anti-proliferation activity in vivo.

Conclusions: The combination of cRGD Nano-MB and US is expected to be a promising strategy for peptide drug delivery and enhancing anti-proliferation and anti-angiogenesis.

Introduction

Both angiogenesis and proliferation of tumor cells are the main features of tumor tissues. Angiogenesis can promote the growth of tumor tissues and metastasis; thus anti-angiogenesis is an effective therapeutic approach with which to treat tumor and prevent the tumor recurrence or metastasis (Carmeliet and Jain 2011; Potente et al. 2011). However, tumor neovascularization only composing of endothelium-dependent vessels (EDV) has been challenged by vasculogenic mimicry (VM) (Du et al. 2014). VM is established by highly aggressive tumor cells to provide sufficient blood perfusion for highly malignant solid tumors, such as ovarian cancer (Sood et al. 2001; Du et al. 2014), breast cancer(Zhang et al. 2014, 2016) and hepatocellular cancer (Yang et al. 2015; Liu et al. 2015). Accumulating evidence has confirmed that VM may represent an independent adverse prognostic factor for 5-year survival, tumor staging and metastasis, and the presence of VM in a tumor correlates with a poor clinical outcome (Sood et al. 2002; Wang et al. 2013). Thus, the efficient anti-angiogenic strategies should not only inhibit EDV but also suppress the formation of VM.

It has been reported that integrin a_vb_3 are preferentially expressed on neovascular endothelial cells and by a wide range of tumors, but are low expressed in normal tissues (Park et al. 2008; Zhan et al. 2010; Luo et

al. 2017). In particular, integrin a_vb_3 inhibitors can induce the apoptosis of the vascular endothelial cells in tumor tissues resulting in anti-tumor effects (Desgrosellier and Cheresh 2010; Chakravarty et al. 2015; Tang et al. 2016). cRGD peptide (cyclic Arg-Gly-Asp) has high affinity with integrin a_vb_3, therefore it can exert a specific inhibitory effect upon EDV (Pasqualini et al. 1997; Jin and Varner 2004). In particular, Wang et al found that cRGD also presented the inhibitory effect on VM formation in cancer cells (Tang et al. 2016). Thus, cRGD exhibits the combination suppressed ability upon EDV and VM formation, thereby possessing the effective anti-proliferative effect upon tumor cells. Over recent decades, nanoparticles (Nano) have presented great prospect for combining and delivering therapeutic agents simultaneously and specifically to tumors due to their enhanced permeability and retention (EPR) effect, diverse surface chemistry and unique pharmacokinetics. Nevertheless, current peptide-based nanoparticle drug delivery platforms have not obtained the expected therapeutic efficacy due to rapid degradation of peptide and relative low tumor accumulation.

Finding effective ways to increase active pharmaceutical agent accumulation in tumor tissues is one of the major challenges for tumor therapy. Ultrasound-targeted microbubble destruction has been a prospective strategy for drug delivery to localize intratumoral drug release and enhance intracellular drug accumulation. Ultrasound (US) combined with microbubbles (MB) can enhance the intracellular drug delivery attributing to the sonoporation of US and inertial cavitation of MB (Zhang et al. 2018; Jing et al. 2019). However, the drug loading ability of MB is relatively limited thereby preventing its application in drug delivery due to the phospholipid MB filled with gas core (Lentacker et al. 2010). It was reported that the loading capacity of MB could be increased by attaching small nanoparticles to the surface of MB. Accordingly, we attempt to design cRGD-based nanoparticles (cRGD Nano) attached to the surface of MB enabling to efficiently deliver cRGD Nano to ovarian cancer cells thereby enhancing its tumor accumulation and improving anti-proliferation and anti-angiogenesis assisted by US. Herein, heparin could react with cRGD to prepare cRGD-H conjugate and then conjugated with biotin to prepare cRGD Nano, and cRGD Nano was subsequently combined with MB to prepare cRGD Nano-MB via avidin-biotin bridge (Scheme 1). The prepared cRGD Nano-MB was further investigated the function of anti-proliferation and anti-angiogenesis for ovarian cancer cells with or without US. To the best of our knowledge, no one has yet developed a cRGD Nano-MB combined with US to deliver cRGD thereby enhancing the cellular uptake ability and efficiently suppressing proliferation and the formation of EDV and VM.

Experimental

Materials

Heparin sodium (Mn = 1.25 kDa, 150 U/mg) was obtained from Sinopharm Chemical Reagent Co. (Shanghai, China). Oregon green488 cadaverine and 1,1'-dioctadecyl-3,3,3',3'-tetramethylindocarbocyanine perchlorate (DiI) were obtained from Invitrogen Co. (USA). 4-dimethylaminopyridine (DMAP), 1-ethyl-3,3-dimethylaminopropylcarbodiimide hydrochloride (EDC), and N-hydroxysuccinimide (NHS) were purchased from Medpep Co. (Shanghai, China). 732 cation-exchange

resins were purchased from Shanpu Co., Ltd. (Shanghai, China). cRGD peptide (Cyclo-Arg-Gly-Asp-D-Tyr-Lys) was synthesized by BoXin Biology Co. Ltd. (Xiamen, China). Succinylated-heparin, Biotin-NH_2 and Biotinylated MB were synthesized in our lab. All other chemicals and reagents were purchased from Sigma Co. (USA). Spectra/Por 3 Dialysis Membrane (MWCO 3,500) was purchased from Pharmacia (Piscataway, NJ). Ultrapure water (Mili-Q, 18 M • W) was used in the experiment.

Preparation of cRGD Nano

Succinylated-heparin (0.050 g) was dissolved by dry DMSO with gentle heating. cRGD peptide (0.006 g), and Biotin-NH2 (0.004 g), EDC (0.04 g, 0.2 mmol) and NHS (0.025 g, 0.2 mmol) were mixed and reacted at room temperature for 24 h. Biotinylated cRGD-H conjugate in solution was then dialyzed with distilled water for 48 h in a dialysis membrane (MWCO 3500) to fabricate cRGD Nano. After lyophilization, biotinylated cRGD-H conjugate (0.22 g) obtained as white powder. Oregon green488-labled biotinylated cRGD-H was prepared by a similar method as that of biotinylated cRGD-H. The amount of cRGD in nanoparticles was measured by bicinchoninic acid (BCA) assay according to the manufacturer's instruction. Folate content was measured by UV method at 366 nm. The loading efficiency of cRGD in cRGD Nano was calculated using the following equation: loading efficiency (%) = (weight of agent in nanoparticles/initial weight of agent) × 100%.

Preparation of cRGD Nano loaded microbubbles (cRGD Nano-MB) and characterization

cRGD Nano-MB was prepared by the described method with minor modifications.(Yin et al. 2013) The biotinylated MB reacted with 500 mL avidin (10 mg/mL) for 10 min at room temperature with gentle shaking. Free avidin were separated from the avidin-bound biotinylated MB by washing for 2 times. And then biotinylated cRGD Nano (50 mL) mixed with avidinylated MB (1 mL) for 15 min with gentle shaking. Free biotinylated cRGD Nano were removed by washing for 2 times. Oregon green488 labled cRGD Nano loaded MB was using similar method. DiI was mixed with MB for 20 min to prepare DiI labeled MB (MB-DiI). To investigate the binding efficiency and construction of NPs-loaded MB, Oregon green488 labled cRGD Nano loaded MB-DiI was visualized using a confocal laser scanning microscope (Olympus FV1000, Japan) with the excitation wavelength of 405 nm for blue channel, 488 nm for green channel and 559 nm for red channel. The ^1H NMR spectra of cRGD-H were recorded on a Bruker-400 MHz NMR in D_2O. Size distributions of cRGD Nano and cRGD Nano-MB were detected by dynamic lighting scattering (DLS) using a Zetasizer Nano-Zs (Malvern Instruments, UK) and Coulter Multisizer Ile (Beckman Coulter, USA), respectively. ^1H NMR spectra of Biotinlyated cRGD-F-H in D2O were detected for structural characterization (Fig. S1).

Cell Culture

Human umbilical cord vein endothelial cells (HUVEC), human ovarian carcinoma SKOV3 cells and human lung carcinoma A549 cells were come from ATCC. All cell lines were cultured in DMEM (Corning, USA)

containing 10% fetal bovine serum (Bioind, Israel) and 100 units/mL penicillin/streptomycin. All cell lines were maintained in humid environment containing 5% CO_2 at 37 ºC.

Ultrasound Setup

Ultrasound-waves were produced from an unfocused single element transducer (Vermon SA, Tours, France) with a center frequency of 1 MHz, driven by a waveform generator (Agilent, City, CA, USA). A power amplifier (ADECE, Artannes sur Indre, France) was generated a pulsed US at acoustic pressure amplitude determined by a calibrated PDVF needle hydrophone (0.2 mm diameter, Precision Acoustics, Dorchester, UK). cRGD Nano-MB were scanned under the transducer (30 s, a center frequency of 1 MHz, 50% duty cycle) and negative peak pressure amplitude for HUVEC cells, SKOV3 cells and A549 cells was 0.7 -1 MPa.

Cellular uptake of cRGD Nano and cRGD Nano-MB with and without US

Oregon green488-labeled cRGD Nano and cRGD Nano-MB were synthesized by the similar procedure. HUVEC, SKOV3 and A549 cells were respectively cultured in 6-well plates (3´ 10^5 cell/well) and incubated for 24 h at 37 ^oC. The culture medium was replaced by fresh medium with Oregon green488 labeled cRGD Nano and cRGD Nano-MB and then followed by US exposure. And the bottom of the plate was drowned in water for acoustic coupling without contaminating the sample in the well of the plate. Meanwhile, the US transducer was submerged in water upward aiming at the plates. HUVEC SKOV3 and A549 cells treated with US under 0.7 MPa-1 MPa for 30 s. The cells were incubated for 4 h and then were washed for three times with cold PBS, detached by 0.02% EDTA-PBS, and suspended in PBS containing 0.1% BSA. The collected cells were analyzed by a FACSort flow cytometer (Becton Dickinson, USA) with 488 nm and cells without any treatment were taken as control.

Confocal laser scanning microscope was used to visualize the cellular uptake of Oregon green488 labeled cRGD Nano and cRGD Nano-MB in HUVEC and SKOV3 cells. The cells were incubated in 6-well plate for 24 h and then the culture medium was replaced with medium containing Oregon green488-labeled cRGD Nano and cRGD Nano-MB with or without US. The ultrasound parameters were the same as the above procedure. The plates were incubated for 4 h at 37 ^oC after US treatment, and cells were washed by PBS and fixed by 4% (w/v) para-formaldehyde solution. The fluorescent images were observed by confocal microscope.

In vitro anti-angiogenesis (anti-EDV and anti-VM) assays

Endothelial tube formation in vitro was conducted by the described method.(Kheirolomoom et al. 2007) Matrigel (50 mL) was added to a 24-well plate and allowed to polymerize. HUVEC cells were suspended in medium with 3´ 10^5 cells/mL, and the cell suspension (0.1 mL) was added to each well coated with Matrigel. And then Cells were treated with cRGD Nano or cRGD Nano-MB (each at an equivalent cRGD dose of 600 mg/mL) with or without US and then incubated for 12 h at 37 ^oC. After that,

the cells were photographed using an inverted light microscope (NiKon ECLPSE 80i system, Japan) and branch points from 4 to 6 high-power fields (200) were counted and averaged.

Matrigel (150 mL) was placed on 24-well plates and allowed to polymerize for 1 h at 37 ^{o}C. 1.5´ 10^4 number of MDA-MB-231 were seeded on the well to observe the ability of capillary-like structure formation. The mild dosage was selected to guarantee its cell viability around 80%. cRGD Nano or cRGD Nano-MB (each at an equivalent cRGD dose of 600 mg/mL) with or without US were added to the cell suspensions. After that, images were photographed using an inverted light microscope after 96 h.

In vivo assessment of angiogenesis using chicken chorioallantoic membrane (CAM)

White Leghorn chicken eggs (South China Agricultural University, Guangzhou) were incubated under routine conditions (constant humidity and 37 ^{o}C) in CAM assay, and a square window was opened in the egg shell at day 3 incubation which exposed the CAM. Gelatin sponges were cut to 1 cm^3 size and placed on the top of the CAM under sterile conditions at day 8. The sponges were then absorbed with cRGD Nano or cRGD Nano-MB (each at an equivalent cRGD dose of 600 mg/mL) with or without US and then they were tested. Sponges with PBS were used as negative controls and each group consisted of three eggs. The blood vessel inhibition ratio was identified as the percentage of treated group vessels area (VA) occupied by the whole area of CAM under the microscopic field. CAMs were observed daily and photographed in vitro at 72 h. Image-Pro Plus 7.0 software was used to automatically assess and quantify the blood vessel areas.

Cell viability detected by MTT assay

HUVEC and SKOV3 cells were separately seeded in 6-well plates (3´ 10^5 cell per well) and incubated for 24 h at 37 ^{o}C. After incubation of 24 h, cRGD Nano or cRGD Nano-MB were added to the medium with drug concentration of 0.06, 0.12, 0.3 and 0.6 mg/mL. The bottom surface of the plate was drowned in water for irradiation and the US transducer was then submerged in water upward aiming at the plates. US condition were set to 0.7 MPa-1 MPa for 30 s and then cells were incubated for 4 h. After that, the cells were washed and trypsinized to transfer 96-well plates with fresh medium for 20 h incubation. The culture medium was replaced with MTT solution and then the cells were further incubated for another 4 h. The medium was replaced by DMSO and the plates were slightly shaken for 10 min. The plates were measured by a microplate reader (Labsystem, Multiskan, Ascent, Finland) at optical absorbance of 570 nm. Cells with PBS were used as control.

In vivo anti-tumor experiments

Athymic nude female nu/nu mice (4–5 weeks old) were injected with 100 mL of SKOV3 cells (1´ 10^6) on the right flank. The tumors were allowed to grow until their size reached between 9 and 25 mm3. Mice were randomly divided into three groups (PBS, cRGD Nano-MB and cRGD Nano-MB+US, n = 5) and injected tail intravenously. The cRGD Nano-MB and cRGD Nano-MB+US (each at an equivalent dose of 150 ug cRGD per mice) were injected at one day intervals. For the cRGD Nano-MB +US group, tumors

were irradiated with US after every injection under the following settings: 1 MHz, 2 % duty cycle, duration of 1 min and intensity of 2 W/cm^2.T umor length (a), width (b) measurements, and body weight were recorded at one day intervals. Tumor volume was calculated according to the formula: V= (a´b^2)/2

Statistical analysis

Statistical analysis was conducted to determine the differences of the experiments. One-way analysis of variance was used to analyze by a statistical program (Statistical Package for the Social Sciences, Version 19.0, SPSS Inc., USA). All the data were performed in triplicate and showed as a mean value with its standard deviation indicated (mean ± SD). Differences were considered the significance at * P < 0.05, * *P < 0.01, * * * P < 0.001.

Results And Discussion

Although nanotechnology-based drug delivery platforms presented promising prospect for delivering therapeutic agents simultaneously and specifically to tumors, the current peptide-based nanoparticles still could not achieve the expected therapeutic efficacy due to the rapid degradation of peptide and their low tumor accumulation. The combination US with MB could enhance the intracellular drug delivery owing to the sonoporation of US and inertial cavitation of MB. Herein, we designed NPs-MB complex using nanoparticles attached to the surface of MB thereby increasing the drug loading capacity of MB and enhancing the intracellular uptake ability of cRGD Nano assisted by US effect. In the cRGD NPs-MB complex, the carboxyl group of succinlyated-heparin was first conjugated with the amine of cRGD to synthesize cRGD- Heparin and then introduced the small amount of biotin to facilitate combination with MB. The cRGD-Biotin-Heparin could be dialyzed to prepare cRGD Nano. And then, cRGD Nano was incorporated with MB by avidin-biotin bridge to create a new drug delivery system cRGD Nano-MB. The design could increase loading capacity of MB, simultaneously enhance cRGD tumor accumulation and improve the bioavailability of cRGD Nano with the aid of US (Scheme 1).

We characterized ^{1}H NMR spectrum of cRGD-Heparin conjugate in D2O. It was observed chemical shift of 6.79 ppm and 7.05 ppm corresponding to cRGD fragment, indicating we prepared successfully cRGD-H conjugate (Figure S1). Due to the small of amount of biotin, it was hard to detect the signal of biotin using 1H NMR. We prepared cRGD-biotin-Heparin conjugate which could present amphiphilic property facilitating to self-assemble into cRGD Nano. Their size distribution and morphology were determined by DLS and TEM. TEM detected they presented approximately spherical shape (Fig. 1a). Also, DLS results displayed the mean diameter of cRGD Nanos was approximately 51 ± 2 nm (Fig. 1b). The content of cRGD was about 14.4% as determined by BCA assay. The amount of cRGD Nano bound to MB was detected by removing the unbound cRGD Nano from MB via centrifugation. We screened the optimal ratio of cRGD Nano and MB by detecting cRGD amount. The loading concentration of cRGD was about 85.2 mg/10^8 MB when 1 mg/mL of cRGD Nano was added to the MB. With the increased cRGD Nano concentration, the drug loading efficiency of cRGD Nano-MB was increased. When the optimal procedure was the mixture of 2 mg/mL of cRGD Nano and 10^8 mg /mL of MB, it could obtain

around 178.7 mg cRGD per 10^8 MB. The size and concentration of cRGD Nano-MB were determined by Coulter Multisizer, and the drug loading efficiency of cRGD Nano-MB was investigated (Tab. 1). In comparison with the method of MB directly carrying free cRGD, our designed method presented higher drug loading efficiency (Kheirolomoom et al. 2007; Lentacker et al. 2010; Wang et al. 2019). To further confirm the successful attachment of cRGD Nano to the surface of MB shells, we prepared Oregon green488 labeled cRGD Nano and DiI encapsulated to MB (Oregon green488-cRGD Nano-MB-DiI). Oregon green488-cRGD Nano was attached to the surface of MB-DiI to prepare Oregon green488-cRGD Nano-MB-DiI via avidin-biotin bridge. Confocal laser scanning microscopy was used to detect two fluorescent signals of Oregon green488 and DiI and we could observed MB morphology in bright field. It clearly showed that the surface of MB was homogeneously covered by green and red fluorescent signals (Fig. 1c), indicating cRGD Nano had ability to patch on the surface of the MB shells.

Recent studies showed that cavitation and sonoporation induced by US could assist drug delivery system to enhance cell membrane permeability thereby facilitating drug accumulation at the specific region (Yan et al. 2013; Li et al. 2018). In this study, we compared the cellular uptake efficiency of cRGD Nano and cRGD Nano-MB with an without US (Fig. 2). Their cellular uptake ability could be affected by US irradiation. It was found that HUVEC and SKOV3 cells treated with cRGD Nano-MB with US displayed the highest cellular uptake efficiency compared to cRGD Nano and cRGD Nano-MB without US. The results demonstrated US irradiation could improve the cellular uptake efficiency of cRGD Nano. cRGD Nano presented the second higher cellular uptake in these cells, while without US exposure cRGD Nano-MB group could not efficiently enter into these cells, which possibly attributed to the its large size. To further confirm the cellular uptake efficiency, these cells treated with cRGD Nano and cRGD Nano-MB with or without US were visualized with a confocal microscope. As shown in Fig. 3, Oregon green488-cRGD Nano were observed in cytoplasm, while the fluorescence of cRGD Nano-MB without US was not stronger than cRGD Nano. It was speculated the increased size of cRGD Nano-MB limited its cellular uptake ability in the absence of US. In comparison, the fluorescence was significantly enhanced when cRGD Nano-MB exposed to US, suggesting the cavitation effect induced by US could improve cellular uptake efficiency of cRGD Nano-MB. The results of confocal images were in accordance with that of flow cytometry. Collectively, the synergistic effect from US irradiation were beneficial to the enhancement of peptide drug delivery.

Anti-EDV effect in vitro and in vivo of cRGD Nano, cRGD Nano-MB with or without US was conducted by using microtube formation experiments of HUVECs and the CAM assay. Regard to the microtube formation experiments of HUVECs, cRGD Nano-MB with US could present best inhibitory ability of microtubule formation (70.3 ± 2% inhibition) than cRGD Nano (48 ± 4% inhibition) and cRGD Nano-MB without US (30.6 ± 7% inhibition) in HUVECs ($P < 0.001$) (Fig. 4a). Regard to the CAM assay,

the untreated CAM displayed a normal pattern of vascularization (29.8 ± 1%, vessel area/CAM area) and cRGD Nano-MB without US could produce slight inhibition (23.5 ± 2%, $P < 0.05$). The blood vessel formation within the allantoic membrane showed that cRGD Nano group presented a significant anti-angiogenic response (18.5 ± 2%, vessel area/CAM area, $P < 0.01$), in comparison spontaneous

angiogenesis was significantly inhibited under cRGD Nano-MB with US (13.8 ± 1.7%, vessel area/CAM area, $P < 0.001$) (Fig. 4b). It was shown the boundaries and capillaries of the CAM disappeared, suggesting that US could help cRGD Nano-MB to present a strong anti-angiogenic response of EDV.

Anti-VM effect in vitro of cRGD Nano and cRGD Nano-MB with or without US was performed by using microtube formation experiments of MDA-MB-231 cells (Fig. 4c). It was shown cRGD Nano-MB with US exhibited preferable destructive effect upon the vessel-like channels (56.9 ± 3% inhibition), while cRGD Nano exhibited better inhibitory effect than cRGD Nano-MB without US. The order of anti-VM effect: cRGD Nano-MB with US> cRGD Nano> cRGD Nano-MB without US. The results indicated US could further assist cRGD Nano-MB to improve the inhibitory ability to VM formation. Collectively, anti-EDV and anti-VM effect were attributed to the ability of cRGD Nano and US could enhance the inhibitory ability.

Accumulating documents reported the cavitation and sonoporation of US could promote the delivery of anticancer drugs, thus the cytotoxicity of drug could be enhanced by US exposure.(Kiessling et al. 2012; Yin et al. 2013; Aw et al. 2016) In this study, we evaluated the cytotoxicity of cRGD Nano, cRGD Nano-MB with or without US in HUVEC and SKOV3 cells. As shown in Fig. 5, blank MB with US could not produce clear cytotoxicity under acoustic pressures of 0.7 MPa-1 MPa for three cells (gray bar). In addition, the cRGD Nano-MB combined with US presented the highest cytotoxicity than that of cRGD Nano and cRGD Nano-MB without US. Meanwhile, cRGD Nano exhibited better the cell death ability than cRGD Nano-MB without US. The results suggested that ultrasound-mediated cavitation contributed to enhance anti-proliferation ability of cRGD Nano.

We then compared their anti-tumor effect of cRGD Nano, cRGD Nano-MB with or without US in the SKOV3 xenograft mouse model. Each treatment group was intravenously injected into mice model using PBS as the control. After the mice were treated with cRGD Nano, cRGD Nano-MB with or without US, tumor growth, neovascularization and the inhibition of proliferation were monitored as shown in Figure 6, US irradiation could significantly enhance the antitumor activity of cRGD Nano-MB; and cRGD Nano presented slightly better anti-tumor activity than cRGD Nano-MB, which was attributed to its larger size. In addition, the body weight of mice in treatment groups was no obvious change, indicating anti-angiogenesis therapy almost had no cytotoxicity in vivo (Figure S). We then detected tumor proliferation and VM expression in tumor tissues using Ki67 and CD34/PAS dual staining (Fig. 6B). The immunohistochemistry results showed cRGD Nano-MB with US exhibited lowest the expression level of Ki67; and the order of Ki67 expression was as followed: PBS> cRGD Nano-MB> cRGD Nano> cRGD Nano-MB+US. CD34/PAS double staining was used to verify VM. VM vessels were negative for CD34 immunostaining, but the walls of these VM vessels were PAS-positive. It was observed the number of VM channels was the fewest in the SKOV3 xenograft treated with cRGD Nano-MB in the presence of US, while cRGD Nano-MB had no significant difference with cRGD Nano. Collectively, the immunohistochemistry results were consistent with that of anti-tumor experiments.

Conclusions

In summary, the combined strategy of cRGD Nano-MB with US could increase peptide bioavailability, enhance drug uptake efficiency and exhibited great anti-tumor effect. The enhancement of anti-proliferation, anti-EDV and anti-VM for cRGD Nano induced from cRGD effect and cavitation triggered by US. It provides a promising strategy for improving bioavailability of peptide in anticancer therapy.

Declarations

Acknowledgments

This work was supported by Hengyang Science and Technology Board Project (No. 2019jh010993); Hunan Provincial Health Commission Project (No. 20200689).

Compliance with ethical standards

Conflict of interest The authors declare no conflict of interest

References

1. Aw MS, Paniwnyk L, Losic D (2016) The progressive role of acoustic cavitation for non-invasive therapies, contrast imaging and blood-tumor permeability enhancement. Expert Opin Drug Deliv 13:1383–1396.
2. Carmeliet P, Jain RK (2011) Molecular mechanisms and clinical applications of angiogenesis. Nature 473:298–307.
3. Chakravarty R, Chakraborty S, Dash A (2015) Molecular Imaging of Breast Cancer: Role of RGD Peptides. Mini Rev Med Chem 15:1073–1094.
4. Desgrosellier JS, Cheresh DA (2010) Integrins in cancer: biological implications and therapeutic opportunities. Nat Rev Cancer 10:9–22.
5. Du J, Sun B, Zhao X, et al (2014) Hypoxia promotes vasculogenic mimicry formation by inducing epithelial-mesenchymal transition in ovarian carcinoma. Gynecol Oncol 133:575–583.
6. Jin H, Varner J (2004) Integrins: roles in cancer development and as treatment targets. Br J Cancer 90:561–565.
7. Jing Y, Xiu-Juan Z, Hong-Jiao C, et al (2019) Ultrasound-targeted microbubble destruction improved the antiangiogenic effect of Endostar in triple-negative breast carcinoma xenografts. J Cancer Res Clin Oncol 145:1191–1200.
8. Kheirolomoom A, Dayton PA, Lum AFH, et al (2007) Acoustically-active microbubbles conjugated to liposomes: characterization of a proposed drug delivery vehicle. J Control Release 118:275–284.
9. Kiessling F, Fokong S, Koczera P, et al (2012) Ultrasound microbubbles for molecular diagnosis, therapy, and theranostics. J Nucl Med 53:345–348.
10. Lentacker I, Geers B, Demeester J, et al (2010) Design and evaluation of doxorubicin-containing microbubbles for ultrasound-triggered doxorubicin delivery: cytotoxicity and mechanisms involved.

Mol Ther 18:101–108.

11. Li Y, Zhang X, Luo W, et al (2018) Dual-functionalized nanoparticles loaded microbubbles for enhancement of drug uptake. Ultrasonics 87:82–90.
12. Liu K, Sun B, Zhao X, et al (2015) Hypoxia promotes vasculogenic mimicry formation by the Twist1-Bmi1 connection in hepatocellular carcinoma. Int J Mol Med 36:783–791.
13. Luo W, Wen G, Yang L, et al (2017) Dual-targeted and pH-sensitive Doxorubicin Prodrug-Microbubble Complex with Ultrasound for Tumor Treatment. Theranostics 7:452–465.
14. Park K, Kim Y-S, Lee GY, et al (2008) Tumor endothelial cell targeted cyclic RGD-modified heparin derivative: inhibition of angiogenesis and tumor growth. Pharm Res 25:2786–2798.
15. Pasqualini R, Koivunen E, Ruoslahti E (1997) Alpha v integrins as receptors for tumor targeting by circulating ligands. Nat Biotechnol 15:542–546.
16. Potente M, Gerhardt H, Carmeliet P (2011) Basic and therapeutic aspects of angiogenesis. Cell 146:873–887.
17. Sood AK, Fletcher MS, Zahn CM, et al (2002) The clinical significance of tumor cell-lined vasculature in ovarian carcinoma: implications for anti-vasculogenic therapy. Cancer Biol Ther 1:661–664.
18. Sood AK, Seftor EA, Fletcher MS, et al (2001) Molecular determinants of ovarian cancer plasticity. Am J Pathol 158:1279–1288.
19. Tang J, Wang J, Fan L, et al (2016) cRGD inhibits vasculogenic mimicry formation by down-regulating uPA expression and reducing EMT in ovarian cancer. Oncotarget 7:24050–24062.
20. Wang S-Y, Ke Y-Q, Lu G-H, et al (2013) Vasculogenic mimicry is a prognostic factor for postoperative survival in patients with glioblastoma. J Neurooncol 112:339–345.
21. Wang Y, Tong L, Wang J, et al (2019) cRGD-functionalized nanoparticles for combination therapy of anti-endothelium dependent vessels and anti-vasculogenic mimicry to inhibit the proliferation of ovarian cancer. Acta Biomater 94:495–504.
22. Yan F, Li L, Deng Z, et al (2013) Paclitaxel-liposome-microbubble complexes as ultrasound-triggered therapeutic drug delivery carriers. J Control Release 166:246–255.
23. Yang Z, Sun B, Li Y, et al (2015) ZEB2 promotes vasculogenic mimicry by TGF-β1 induced epithelial-to-mesenchymal transition in hepatocellular carcinoma. Exp Mol Pathol 98:352–359.
24. Yin T, Wang P, Li J, et al (2013) Ultrasound-sensitive siRNA-loaded nanobubbles formed by hetero-assembly of polymeric micelles and liposomes and their therapeutic effect in gliomas. Biomaterials 34:4532–4543.
25. Zhan C, Gu B, Xie C, et al (2010) Cyclic RGD conjugated poly(ethylene glycol)-co-poly(lactic acid) micelle enhances paclitaxel anti-glioblastoma effect. J Control Release 143:136–142.
26. Zhang D, Sun B, Zhao X, et al (2014) Twist1 expression induced by sunitinib accelerates tumor cell vasculogenic mimicry by increasing the population of CD133+ cells in triple-negative breast cancer. Mol Cancer 13:207.

27. Zhang J, Qiao L, Liang N, et al (2016) Vasculogenic mimicry and tumor metastasis. J BUON 21:533–541
28. Zhang N, Yan F, Liang X, et al (2018) Localized delivery of curcumin into brain with polysorbate 80-modified cerasomes by ultrasound-targeted microbubble destruction for improved Parkinson's disease therapy. Theranostics 8:2264–2277.

Tables

Table 1 Loading efficiency of cRGD Nano-MB

Concentration of cRGD Nano (mg/mL)	Loaded cRGD (mg/10^8 MB)	Mean diameter of cRGD Nano-MB (mm)
1	85.2 ± 0.5	2.24 ± 0.7
2	178.7 ± 1.8	2.3 ± 0.8
3	172.1 ± 0.3	2.27 ± 0.83

Schemes

Scheme 1 is available in the Supplemental Files section

Figures

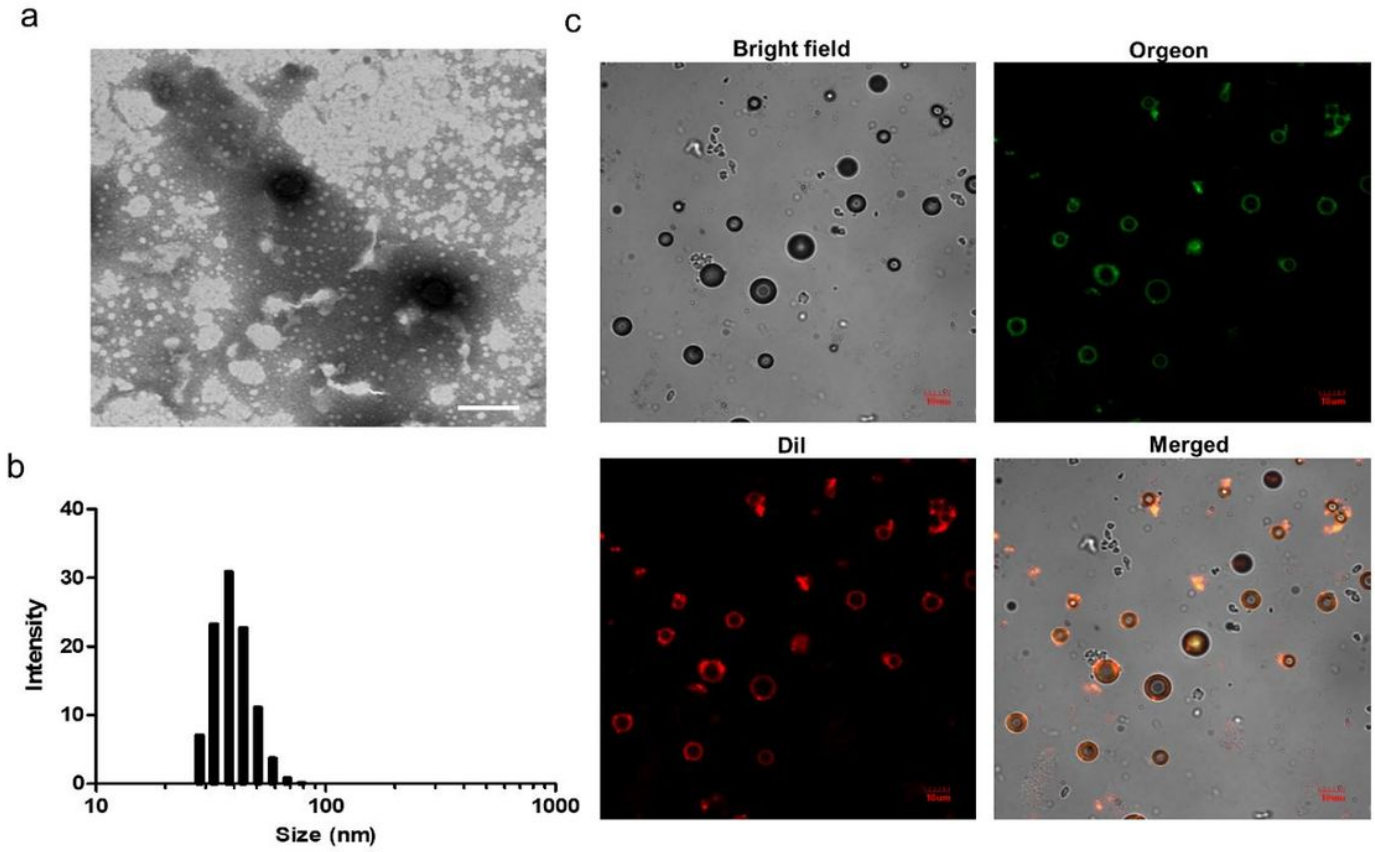

Figure 1

(**a**) Transmission electron microscopy photograph of cRGD-Nano (scale bar: 100 nm); (**b**) Size distribution of cRGD-Nano as measure by DLS; (**c**) Confocal laser scanning microscopy images of Oregon green488-cRGD Nano-MB-DiI and corresponding merged image with bright field (right) (scale bar: 10 mm).

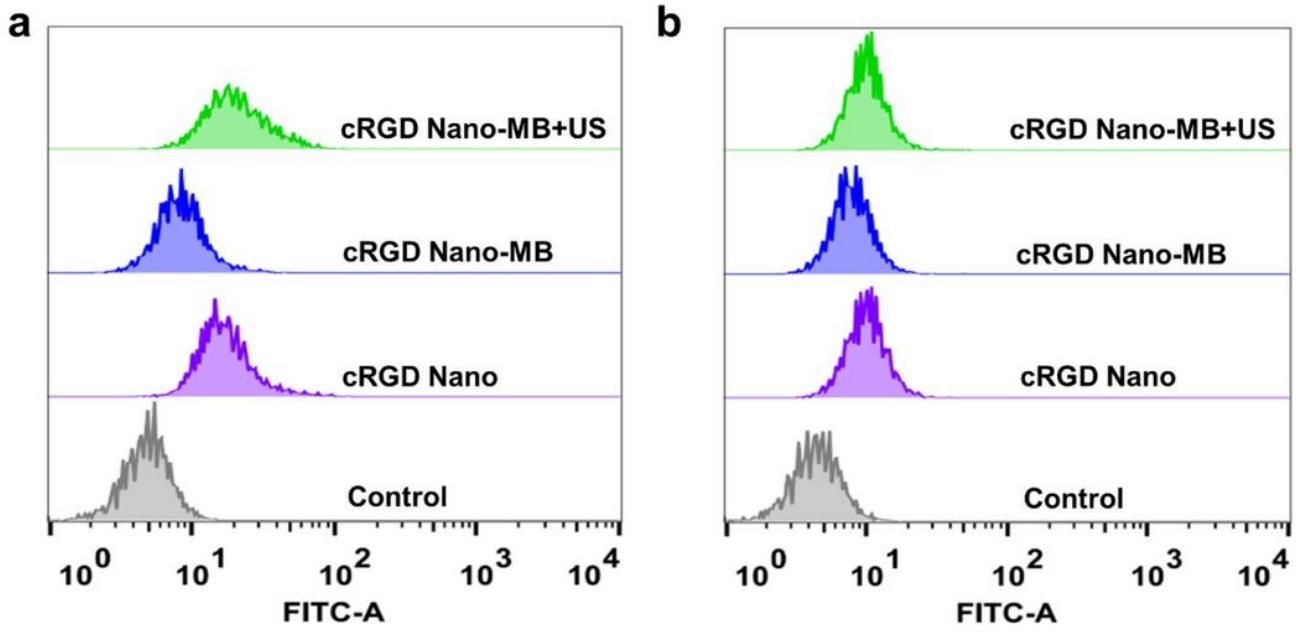

Figure 2

Cellular uptake extends for (**a**) HUVEC cells and (**b**) SKOV3 cells treated with cRGD Nano and cRGD Nano-MB in the presence of or in the absence of US.

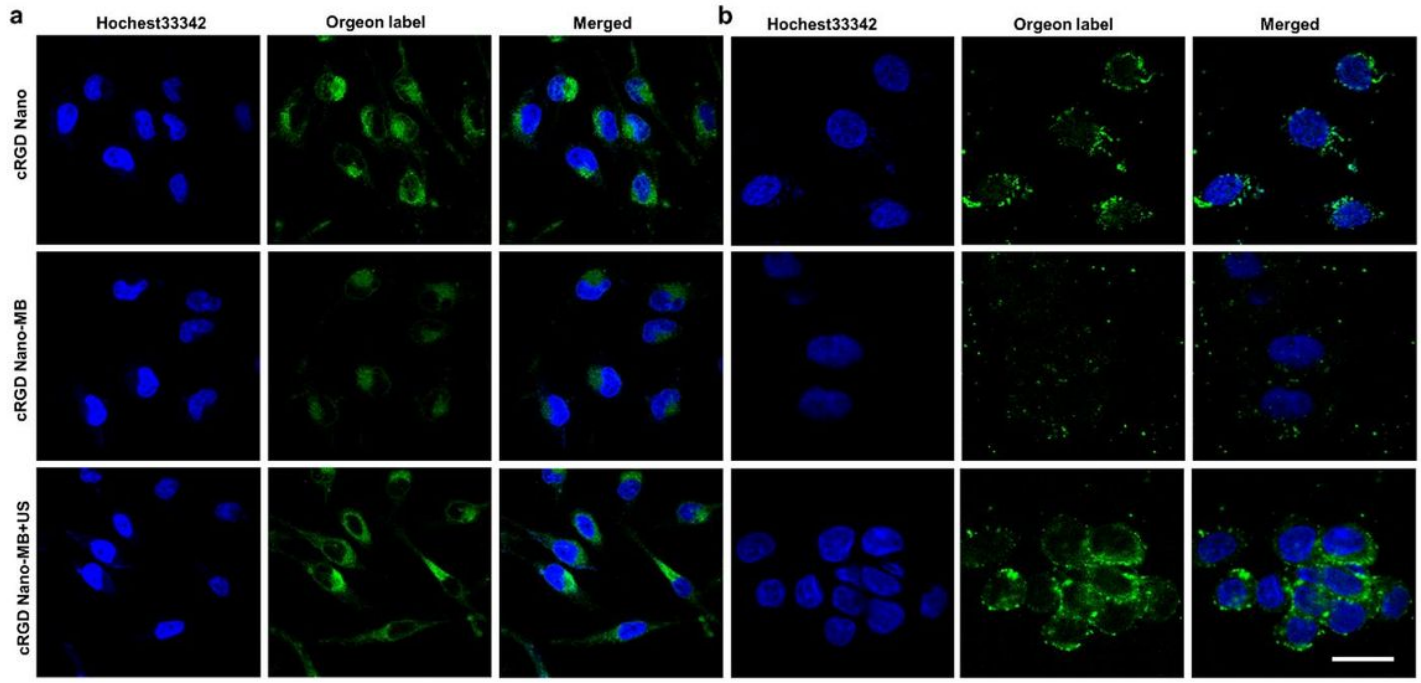

Figure 3

Confocal microscopic images of (**a**) HUVEC cells and (**b**) SKOV3 cells after 4 h incubation with cRGD Nano and cRGD Nano-MB in the presence or in the absence of US. Scale bar: 20 mm.

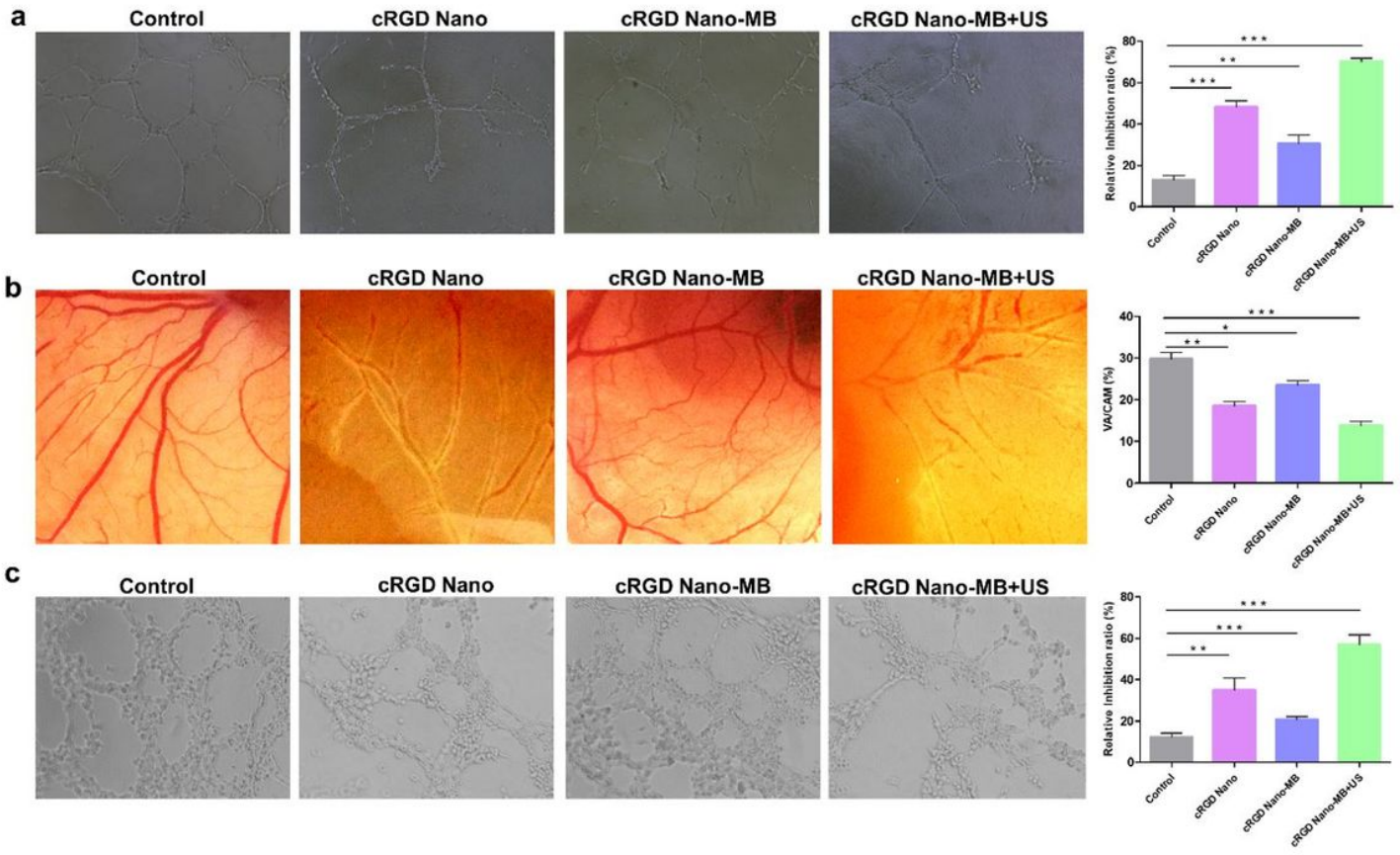

Figure 4

Anti-angiogenesis assays of (**a**) microtube formation experiments of HUVEC cells, (**b**) chorioallantoic membrane, and (**c**) 3D cultures of SKOV3 cells cRGD Nano and cRGD Nano-MB in the presence of US or in the absence of US. (*P < 0.05, **P < 0.01, ***P < 0.001.)

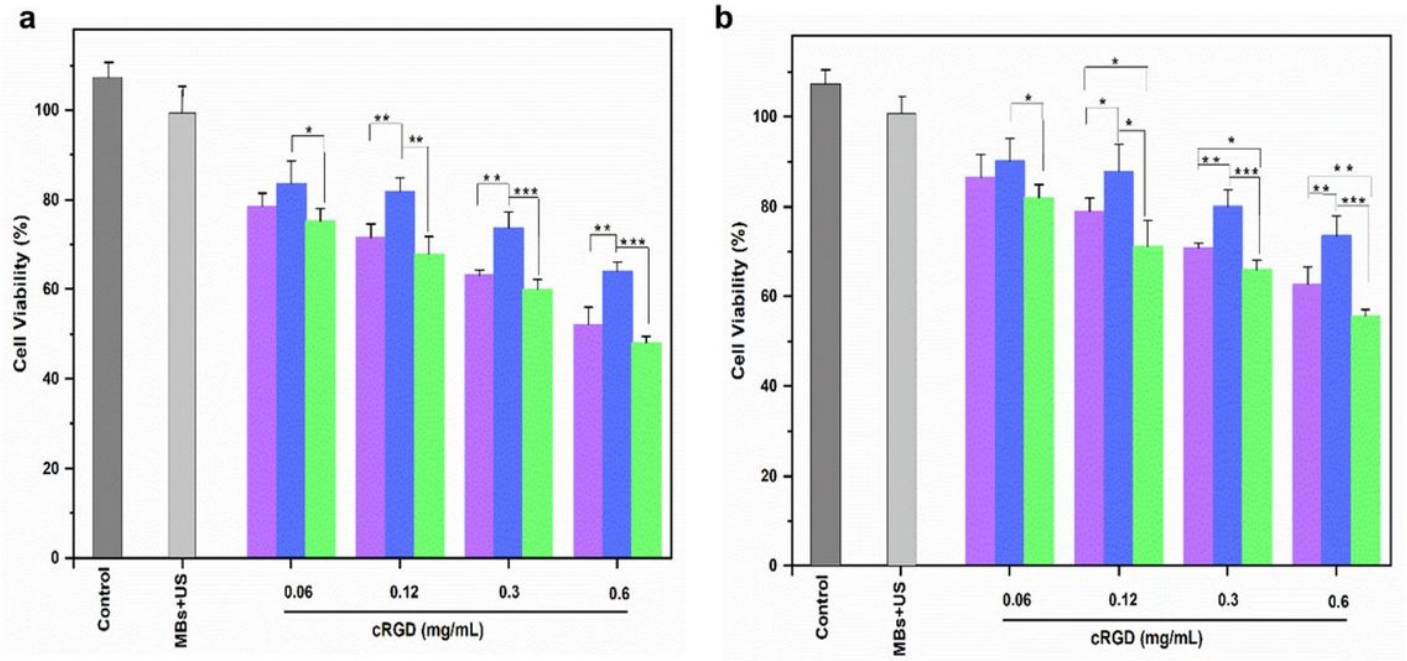

Figure 5

Cell viability of (**a**) HUVEC cells and (**b**) SKOV3 cells after treatment with cRGD Nano (■) and cRGD Nano-MB in the presence of US (■) or in the absence of US (■) for 48 h. (*P < 0.05, **P < 0.01, ***P < 0.001.)

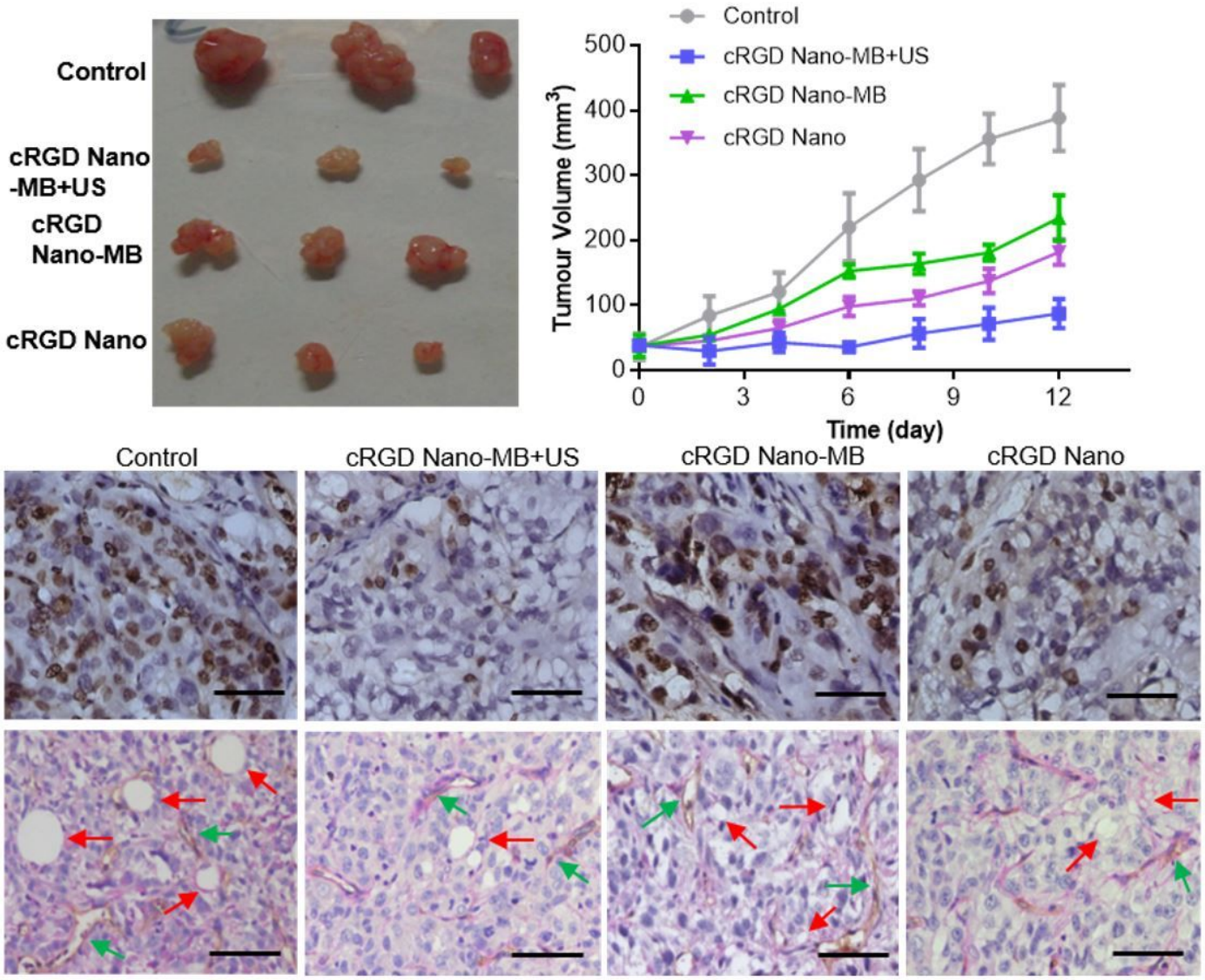

Figure 6

(**a**) In vivo anti-tumor effect of cRGD Nano-MB with or without MB and cRGD Nano in SKOV3 xenograft tumor models (n=3). (**b**) Tumor tissues of different treatment groups were immunostained with Ki67 for cell proliferation and with CD34/PAS, red and green arrows represented VM and EDV, respectively. (*P < 0.05, **P < 0.01, ***P < 0.001.)

Supplementary Files

This is a list of supplementary files associated with this preprint. Click to download.

- Supportinginformation20211018.docx
- Scheme1.jpg